Academic Journal of Science and Technology
ISSN: 2771-3032 | Vol. 14, No. 1, 2025

Sealing Performance Analysis of End Spring Packer

Bojun Xu[1, *]

[1] College of Mechanical Engineering, Xi 'an Shiyou University, Xi 'an 710000, China
[*] Corresponding author: Bojun Xu (Email: xubjxsyu@163.com)

Abstract: Oil exploitation tends to occurs in high-temperature and high-pressure environments, leading to sealing failure of rubber cylinders after long-time operation. To address this challenge, a spring-embedded shoulder protection packer rubber cylinder, made from metal rubber, was specifically designed to enhance the sealing performance under these demanding conditions. The superelastic model was selected by the superelastic theory analysis, and the rubber material parameters were obtained by the curve fitting of uniaxial tensile test, and the sealing performance of the rubber cylinder was analyzed by finite element calculation. The results show that the stability of Yeoh 3-order model is good through theoretical analysis. The YEOH3-order model is selected to calculate the end spring at five different temperatures, proving that it can work normally at 65℃~204℃, providing data support for engineering applications.

Keywords: Packer rubber cylinder; Sealing performance; Contact stress.

1. Introduction

The protection packer is one of the most important tools in oil exploitation and downhole operation, supporting both the regular flow of oil extraction and the effective implementation of downhole technologies. The packer rubber cylinder plays a key role in the protection packer, providing essential functions, such as isolating gas and oil, enhancing fracturing effect, preventing wellbore leakage, and ensuring the wellbore stability [1-2]. As oil exploration gradually moves toward high-temperature and high-pressure environment, the operating conditions for packer rubber cylinders become more severe in downhole. These rubber cylinders must not only function for extended periods underground but also endure extreme external conditions, including high temperatures, elevated pressures, and harsh corrosive forces. Prolonged operation causes degradation of the rubber cylinder's performance, often leading to sealing failures that disrupt downhole activities. In critical cases, such failures can result in safety incidents and significant economic losses [3-4].

To address the situation of sealing failure in packer rubber cylinders under high-temperature and high-pressure downhole conditions, researchers have investigated the influence of the structural design and rubber materials composition on the performance of the packer rubber cylinders. Focusing on rubber material properties, Liu et al. [5] conducted tensile tests on three commonly used rubber materials to assess their suitability for packer rubber cylinders' requirements. With specified wall thickness and radial clearance, applying ultimate pressure loads maintained the rubber cylinder within a safe operating state, where the sealing width closely aligned with the rubber cylinder's contact length, ensuring effective sealing performance. Addressing the harsh downhole conditions, Wang [6] enhanced the corrosion resistance of rubber cylinder by optimizing its rubber material, achieving a packer rubber cylinder capable of withstanding temperatures up to 154 °C, pressure resistance under 79 MPa, and providing sustained sealing performance. Jin [7] analyzed the sealing performance of the packer rubber cylinder composed of AFLAS and KALREZ rubber materials, thereby identifying the optimal temperature and initial setting pressure ranges for maximum sealing effectiveness. Subsequently, he developed constitutive relationships for these two rubber materials using the Mooney-Rivlin model with the reference to temperature effects. They also analyzed the sealing performance of the optimized packers featuring rubber cylinder made from AFLAS and KALREZ rubber materials, offering meaningful insights into the optimization of packer's structure [8]. Hu et al analyzed the sealing performance coefficients and other factors of several rubber materials, and selected the best rubber material to provide reference for selecting materials for rubber cylinders[9].

On the other side, Zhang and his teammates [10] modified the nitrile rubber and fluoroelastomer models, enabling more accurate evaluation on rubber materials' performance, thus providing design perspectives for high-temperature applications. Takahashi et al. [11] tested uniaxial tensile and compressive performance of two dissolvable rubber materials, 80SHA and 90SHA, as well as 80SHA nitrile rubber at 66 °C. They found that dissolvable rubber materials demonstrated superior sealing performance compared to nitrile rubber, which exhibited a higher failure probability. The rubber cylinder structure designed in their study withstands pressures up to 100 MPa. Additionally, some researchers have focused on the structural modifications of the rubber cylinder to facilitate its resistance for high-temperature and high-pressure environments in downhole. Some innovate structure, including shoulder-enhanced designs and M-type rubber cylinder, have enabled rubber cylinder to operate effectively under the condition of 154 °C and 79 MPa [12-13]. Zhang et al. [14] tried to addressed shoulder protrusion issues by designing special-shaped rubber cylinder with various structures. Their simulation results indicated that the right-angle trapezoidal dual-layer rubber cylinder with sloped surface support exhibited significantly improved sealing performance over the traditional rubber cylinder and eliminated shoulder protrusion. Moreover, they further developed a nano-fluidic self-pyrolyzing rubber cylinder, which meets pressure resistance and sealing requirements, outperforming other traditional rubber cylinder [15]. Zheng et al conducted stress relaxation experiments on hydrogenated nitrile rubber at two different temperatures and concluded that

as the temperature increased, the contact stress decreased significantly, providing a theoretical and experimental basis for the design of packers[16]. Polonsky and colleges [17] put forward a new-designed anti-shoulder protrusion structure based on the self-sealing effect of conical rubber, which effectively reduced shoulder protrusion and minimized stress concentration in the shoulder area. This design can also increase the compression level of the rubber cylinder, enhancing the contact stress on both primary and secondary sealing surfaces. Lan [18] used finite element software to numerically optimize the structures of packer rubber cylinders made from two different materials, with their findings verified experimentally. They further identified the weakest points in the designed structure through simulation and optimization. Additionally, some researchers developed an evaluation system for packer sealing performance, thereby establishing an automated high-temperature packer sealing system simulation platform based on this system. This platform enables effective prediction of the packer's sealing performance [19]. Liu et al improved the structure of the recyclable packer rubber cylinder to adapt to the high temperature environment underground [20].

Based on the above research results, this paper firstly selects the appropriate hyperelastic model by analyzing the hyperelastic theory, and obtains the rubber material parameters at five groups of temperatures through the uniaxial tensile test results. The sealing performance of the end spring type rubber cylinder at different temperatures is calculated by finite element method, and its advantages in sealing are analyzed.

2. Introduction to Constitutive Model of Hyperelastic Materials

The mechanical properties of non-metallic materials such as rubber and metal materials have great differences, such as large elastic deformation, incompressibility, viscoelasticity and so on. These materials are collectively referred to as hyperelastic materials, and the mechanical models describing such materials are called hyperelastic models. Several common hyperelastic models are described below.

2.1. Mooney-Rivlin hyperelastic model

$$W = \sum_{i+J=N}^{N} C_{ij} (\bar{I}_1 - 3)^i (\bar{I}_2 - 3)^j + \sum_{k=1}^{N} \frac{1}{D_k} (J-1)^{2k} \quad (1)$$

The following is an analysis based on parameters 2, 5 of the Mooney-Rivlin model.

2.1.1. 2 parameter Mooney-Rivlin model

When N=1 in equation (1-1), the model is reduced to a two-parameter Mooney-Rivlin model, whose strain energy function expression is as follows:

$$W = C_{10}(\bar{I}_1 - 3) + C_{10}(\bar{I}_2 - 3) + \frac{1}{D_1}(J-1)^2 \quad (2)$$

Where C_{10} and C_{01} are the shear modulus of the material, d is the incompressible coefficient, $\bar{I}_1$ is the invariant of the first strain tensor, $\bar{I}_2$ is the invariant of the second strain tensor, *J* is the volume ratio before and after deformation, and *J*=1 when the material is incompressible.

By taking the partial derivation of the second-order strain energy function W into equation (1-2), the rubber superelastic constitutive relation of the second-order Mooney-Rivlin model under uniaxial tensile test can be obtained:

$$\sigma = 2C_{10}(\lambda - \lambda^{-2}) + 2C_{01}(1 - \lambda^{-3}) \quad (3)$$

Where σ is the stress, λ is the elongation ratio, and both σ and λ are measured by tensile tests.

In the 2-parameter model, when $C_{01} = 0$, the Neo-Hookean model is simplified. The non-zeroC_{01} term makes the deformation prediction under uniaxial tensile stress more accurate, but the model cannot accurately simulate the multi-axial stress data, or the data obtained from a certain deformation test, and can not be used to predict other types of deformation. At the same time, the shear modulus of the 2-parameter model is a constant coefficient, which is not suitable for the simulation of carbon black filler vulcanized rubber. C_{10} and C_{01} are positive definite constants. For most rubbers, a reasonable approximation can be obtained within 150% of strain when $C_{10}/C_{01} \approx 0.1 \sim 0.2$

2.1.2. 5 parameter Mooney-Rivlin model

When N=2 in equation (1-1), the model is reduced to a 5-parameter Mooney-Rivlin model, whose strain energy function is expressed as follows:

$$W = C_{10}(\bar{I}_1 - 3) + C_{01}(\bar{I}_2 - 3) + C_{20}(\bar{I}_1 - 3)^2 + C_{11}(\bar{I}_1 - 3)(\bar{I}_2 - 3) + C_{02}(\bar{I}_2 - 3)^2 + \frac{1}{D_1}(J-1)^2 \quad (4)$$

Where C_{10}、C_{10}、C_{20}、$C_{11}$and C_{02} are the shear modulus of the material, D_1 is the incompressible coefficient, $\bar{I}_1$ is the invariant of the first strain tensor, and $\bar{I}_2$ is the invariant of the second strain tensor. When the material is incompressible, *J*=1.

2.2. Yeoh hyperelastic model

Yeoh model is a kind of hyperelastic model which is widely used. The elastic strain energy function is used to describe this model. The elastic strain energy function of Yeoh model is as follows:

$$W = \sum_{i=1}^{N} C_{i0} (\bar{I}_1 - 3)^i + \sum_{k=1}^{N} \frac{1}{D_k} (J-1)^{2k} \quad (5)$$

Where $\bar{I}_1$ is the first strain tensor invariant. N is the order, C_{i0} is the shear modulus of the material, and D_k is the incompressible coefficient. When the material is incompressible, *J*=1.

It can be seen from the strain energy function that the Yeoh model is very similar to the Mooney-Rivlin model and belongs to the polynomial form family. At the same order, the Yeoh model is much simpler than the Mooney-Rivlin model because the invariants of the second deformation tensor are not taken into account, but the term with incompressible coefficient D_k will have higher order complexity. At the same time, the initial shear modulus is $2 \times C_{10}$ and the initial modulus is $2/D_1$. To ensure that the initial shear modulus is positive, the parameter C_{10} must be greater than 0.

Although the number of orders N can be large, it is used in practical applications at most three orders. Because when N=1, it's equivalent to the Neo-Hookean model. Therefore, it is generally recommended to use the third-order Yeoh model with N=3, and the third-order strain energy function is:

$$W = C_{10}(I_1 - 3) + C_{20}(I_1 - 3)^2 + C_{30}(I_1 - 3)^3 + \frac{1}{D_1}(J-1)^2 \quad (6)$$

Yeoh model has obvious characteristics, simple and few parameters. Reasonable numerical results can be obtained with very little test data, and the input parameters can be obtained only through tensile test. At the same time, the described deformation range is wide, and reasonable results can be obtained in uniaxial tensile and shear deformation tests. The higher-order version can describe the shear modulus characteristics of carbon black-filled rubber.

At the same time, Yeoh model also has some shortcomings, there will be deviation in predicting the stress-strain relationship of equal biaxial tensile, and there will be a large deviation in dealing with complex comprehensive strain. At the same time, it is necessary to select parameters carefully under the condition of small strain. In the small strain zone, there will be deviations in Yeoh model and test data, but this deviation is not serious for finite element analysis, because the stress in the small strain zone is very small, and although the relative error may be large, the absolute error is small. Since the Yeoh model can obtain data through tensile test and obtain reasonable results when simulating large deformation conditions, the Yeoh third-order model is used for subsequent simulation calculation.

3. Mechanical Properties Analysis of End Spring Packer Cartridge

3.1. Establish a two-dimensional model of spring shoulder packer cartridge

Considering that the traditional packer casing cannot be fully compressed and deformed, the end-spring packer casing is designed, and its model diagram is shown in Figure 1.

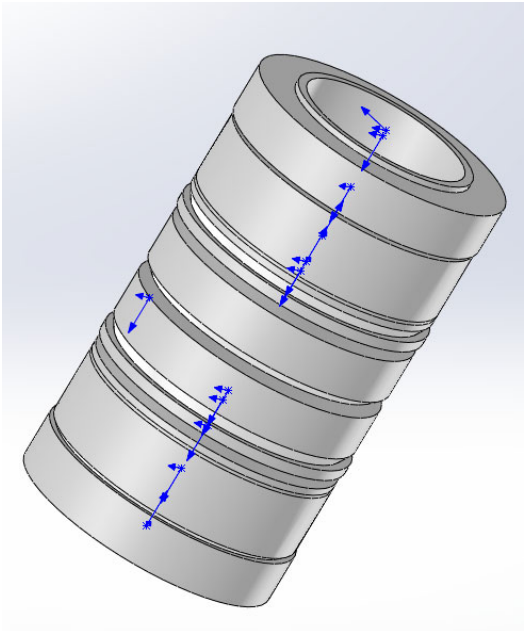

Figure 1. End spring packer cartridge model

The packer adopts a symmetrical structure. From top to bottom, the packer consists of a pressure ring, an edge rubber cylinder, a spacer ring, a middle rubber cylinder, a spacer ring, an edge rubber cylinder, and a pressure ring. Figure 2 shows the cross sections of the packer.

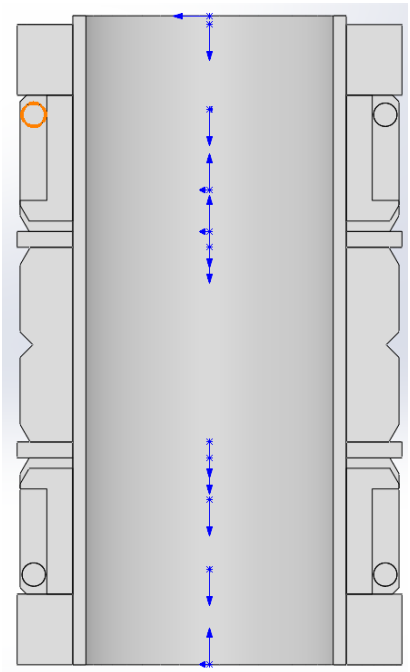

Figure 2. End spring packer cartridge profile

After the model is established, it is necessary to assign material attributes to each component, and 20CrNiMo steel material supports the support ring and shoulder and guard ring. The elastic modulus of 20CrNiMo is E=2.08×10^11 N/m^2, Poisson's ratio λ=0.295, and the density is 7.87×10^3kg/m^2. According to the above theoretical analysis, Yeoh third-order model was selected for rubber materials, and the material parameter values were solved according to curve fitting. The material parameters at different temperatures were shown in the following table 1.

Table 1. Material parameters of Yeoh third-order model at different temperatures

Temperature	C_{10}	C_{20}	C_{30}
65℃	0.89907	0.041931	-0.0008959
100℃	1.0998	0.14942	-0.01768
150℃	0.4854	-0.0012465	0.0012619
177℃	0.93651	0.013589	0.000081062
204℃	0.56278	0.026089	0.0014116

After assigning material attributes to each component, the complete packer Assembly cross-section model can be obtained by assembling in the ABAQUS/Assembly module

After assembly is complete, the contact conditions of the model need to be defined in the interaction module. After defining the contact properties, the boundary conditions of the model are set in the ABAQUS/Load module. According to the actual working conditions, the axial setting force is applied on the surface of the upper support ring of the packer, and the loading amplitude is linearly loaded. After the pressure is set, each inner wall is set as the fixed support constraint in the boundary condition management. This is mainly achieved through the rigid reference point of the constraint setting. At the same time, considering that the deformation of the compression ring and the spacer ring is very small during the loading process, this study set them as rigid bodies during the loading process, so as to observe the stress state of rubber more directly. In addition, in order to monitor the contact stress of the packer, a reference point is placed at a certain interval on the outer wall of the packer to record the contact

force between the packer and the outer wall. The contact force can be used to obtain the overall contact pressure of the packer. After the boundary conditions were set, each component of the packer was meshed. It should be noted that due to the large deformation of the new structure, some mesh units were locally densified in the contact area. In addition, in order to increase the stability of the grid, part of the grid is divided into triangular grids to increase the convergence of the calculation.

3.2. Influence of setting load on axial compression distance of spring shoulder packer

In this paper, the finite element calculation of the end spring packer rubber barrel is carried out to investigate the relationship between the compression distance of the rubber barrel and the contact stress between the rubber barrel and casing under the setting load of 10~50kN. Figure. 3~7 shows the deformation cloud map of the rubber cylinder under different setting loads at 65℃ -204 ℃. It can be seen from the figure that the axial compression distance of the rubber cylinder increases with the increase of setting load at the same temperature.

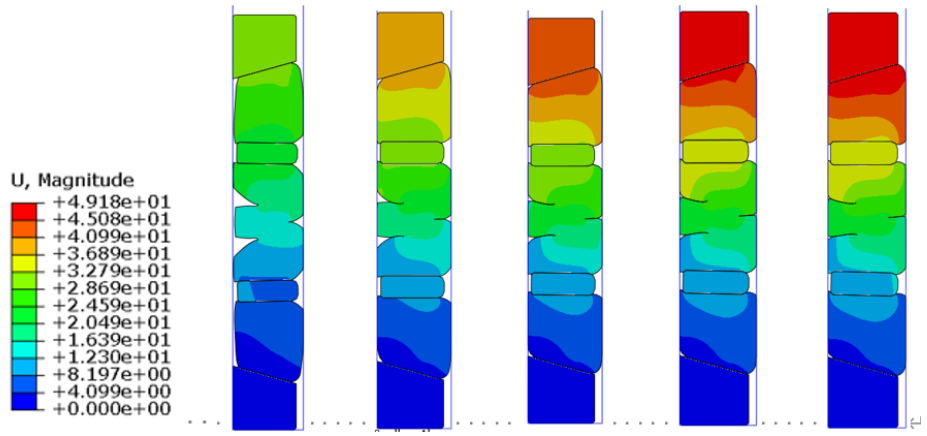

Figure 3. Cloud map of changes of rubber cylinder deformation with setting load at 65℃

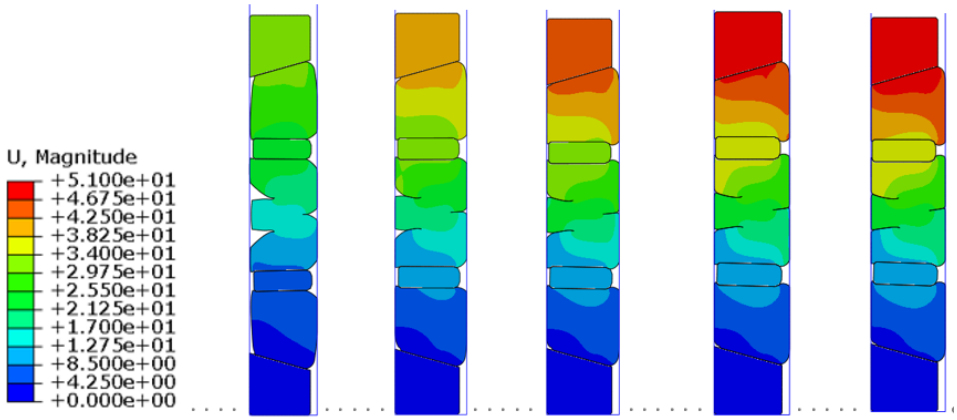

Figure 4. Cloud map of changes of rubber cylinder deformation with setting load at 100℃

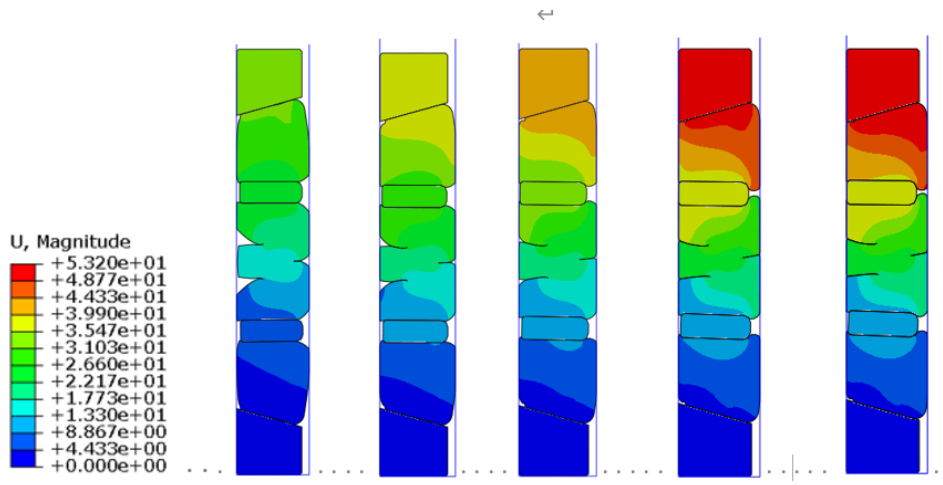

Figure 5. Cloud map of changes of rubber cylinder deformation with setting load at 150℃

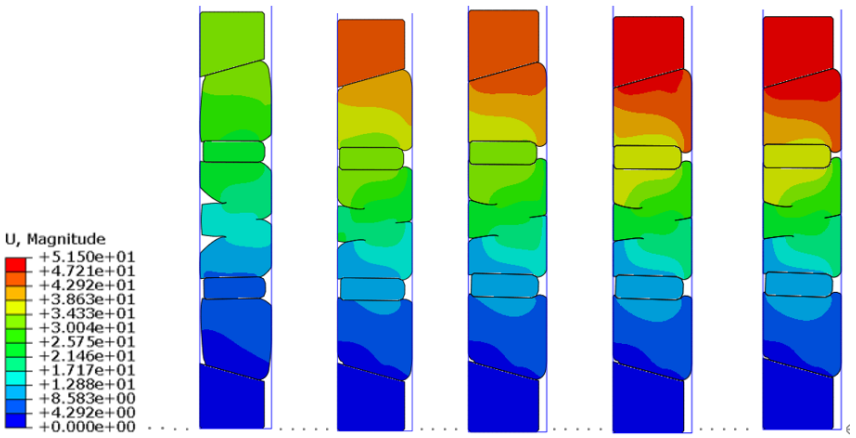

Figure 6. Cloud map of changes of rubber cylinder deformation with setting load at 177℃

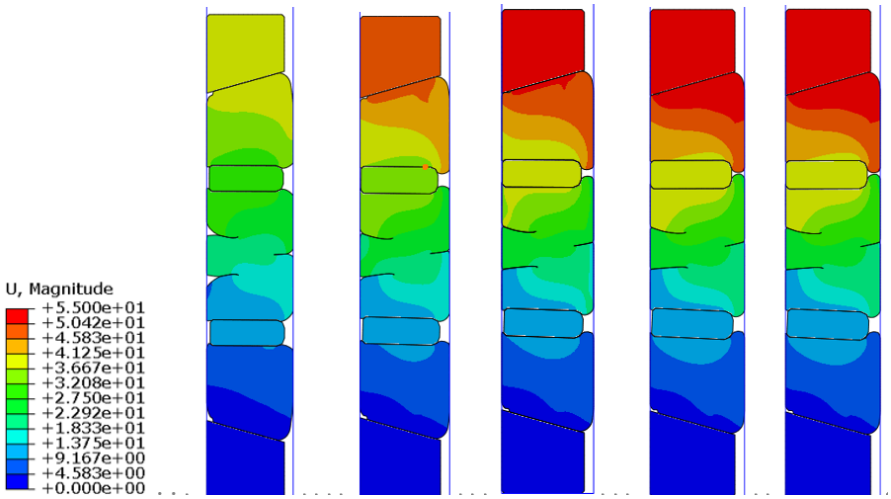

Figure 7. Cloud map of changes of rubber cylinder deformation with setting load at 204℃

The maximum axial displacement of the rubber cylinder under different setting loads at each group of temperatures was extracted and plotted as a curve to obtain the relationship between setting loads and axial compression distance, and then the temperature curves of the five groups were integrated, as shown in Figure 8.

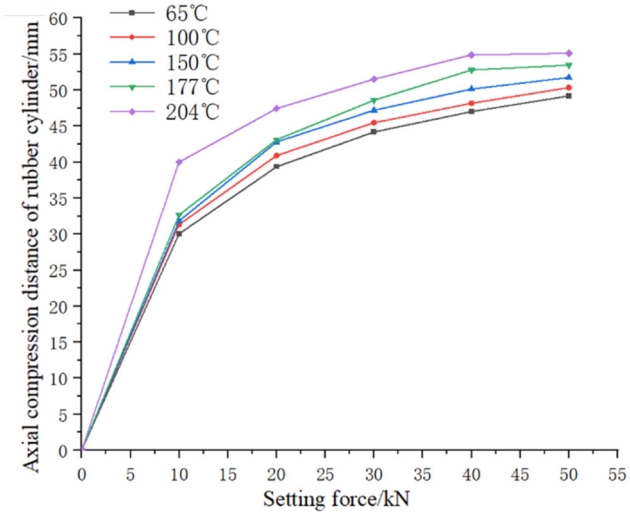

Figure 8. Diagram of the relationship between setting load and axial compression distance of bridge plug cylinder at five groups of temperature

As can be seen from Figure.8, the axial compression distance of the rubber cylinder shows a non-linear increase trend with the increase of setting load. When the setting load is 10~40kN, the axial compression distance of the rubber cylinder increases rapidly with the increase of the setting load, indicating that the rubber cylinder is in a state of free deformation at this time, and the rubber cylinder is not set. When the setting load is 40~50kN, the growth trend of the axial compression distance of the rubber cylinder is gradually gradual, indicating that the rubber cylinder is in the setting stage at this time. With the increase of temperature, the axial compression distance of the rubber cylinder gradually

increased, indicating that with the increase of temperature, the performance of the rubber material weakened, and the hardness of the rubber cylinder gradually decreased with the increase of temperature.

3.3. Establish a two-dimensional model of spring shoulder packer cartridge

Figure 9~13 shows the contact stress distribution of the rubber cylinder under different setting loads at 65℃ -204 ℃. It can be seen from the figure that at the same temperature, when the setting load is 10kN, the rubber cylinder and casing begin to contact, and the contact stress occurs on the outer surface of the rubber cylinder. With the increase of setting load, the contact stress on the outer surface of the rubber cylinder gradually increases, and the contact stress area on the side wall of the rubber cylinder also increases, indicating that the contact area between the rubber cylinder and the casing also increases. Due to the three-cylinder structure of the rubber cylinder, the setting load is applied to the upper spacer ring at the same time, resulting in the contact stress of the upper rubber cylinder is greater than that of the middle rubber cylinder and the lower rubber cylinder, which shows that the upper rubber cylinder mainly bears the sealing requirements. At the same time, due to the existence of the spring shoulder guard, there is no shoulder protrusion phenomenon on the shoulder of the rubber cylinder. Due to the design of the rubber cylinder, there is an annulus inside. With the increase of setting load, the rubber cylinder is further compressed and filled with the gap of the rubber cylinder structure, so that the rubber cylinder can be fully deformed.

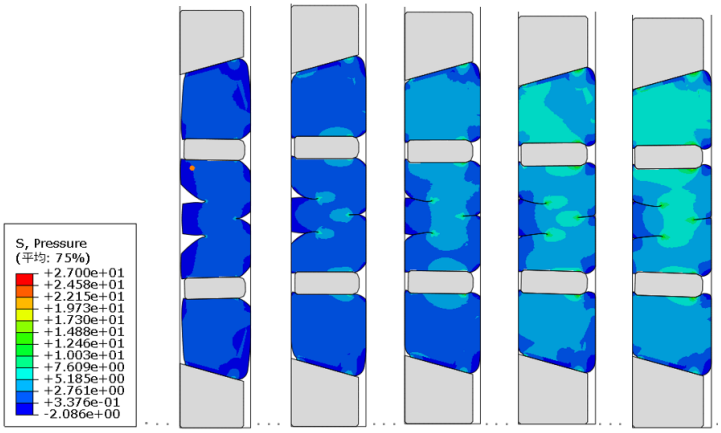

Figure 9. Cloud diagram of change of contact stress of 65℃ rubber cylinder with setting load

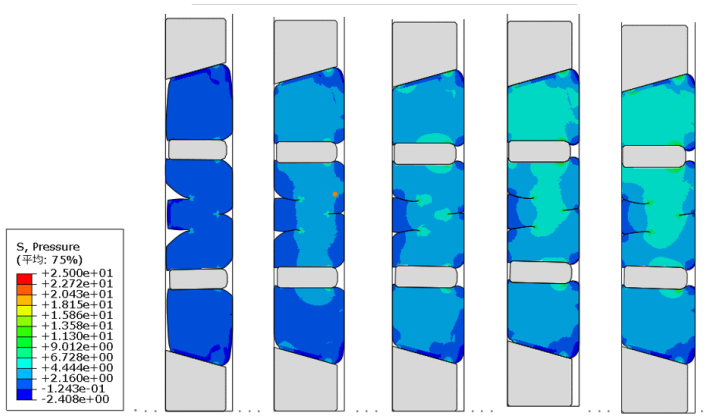

Figure 10. Cloud diagram of change of contact stress of 100℃ rubber cylinder with setting load

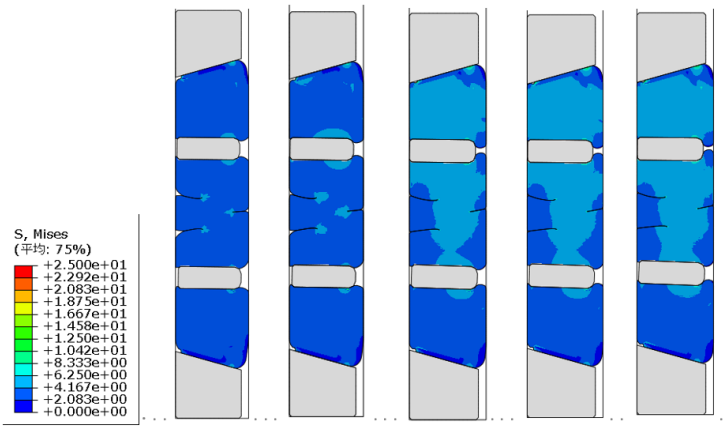

Figure 11. Cloud diagram of change of contact stress of 150℃ rubber cylinder with setting load

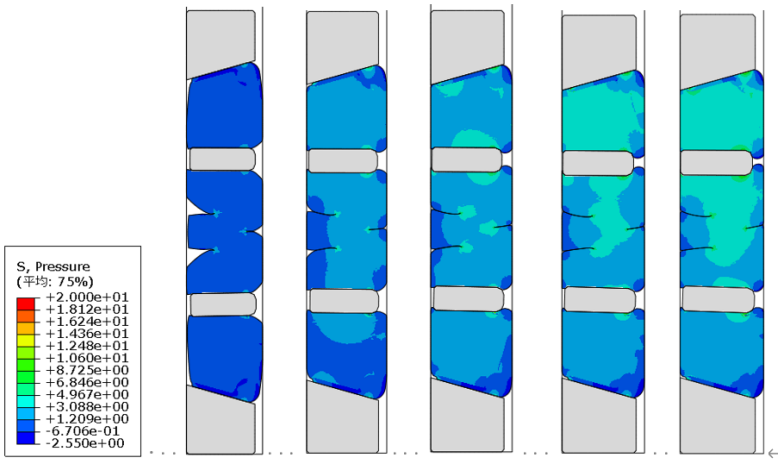

Figure 12. Cloud diagram of change of contact stress of 177℃ rubber cylinder with setting load

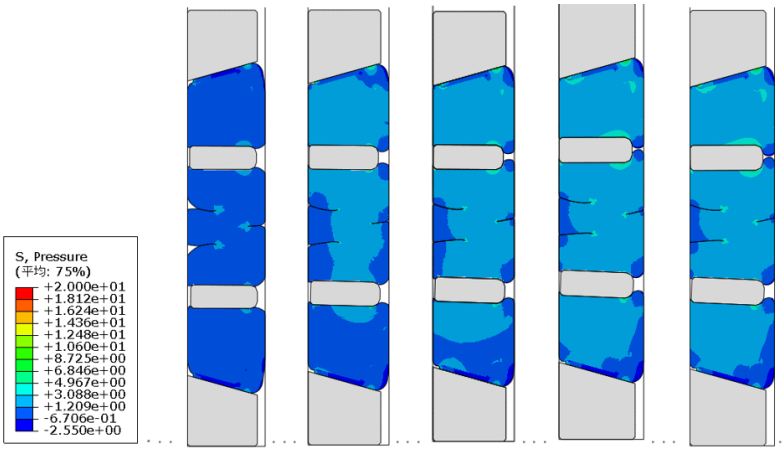

Figure 13. Cloud diagram of change of contact stress of 204℃ rubber cylinder with setting load

Due to the special structure of the rubber cylinder, and it is not completely set at 10kN, there is a gap in the middle of the cloud image, and the stress is 0. With the continuous increase of the contact stress, the rubber cylinder is fully in contact with the casing, and the phenomenon of the stress is 0 disappears. The setting load of the lower rubber cylinder is small, and the contact stress between the rubber cylinder and the casing is less than that of the upper middle rubber cylinder. In the contact process between the rubber cylinder and the casing, with the increase of the load, the middle part of the rubber cylinder first contacts the casing. Therefore, when the load is small, the maximum contact stress between the rubber cylinder and the casing is mainly concentrated in the middle part of the rubber cylinder.

With the increase of temperature, the performance of rubber material weakens, the average contact stress of the rubber cylinder decreases from 10MPa to 2MPa, and the sealing performance decreases. There is no shoulder protrusion during the whole setting process. At the same time, the contact area between the upper end of the middle rubber cylinder and the metal spacer ring is estimated to be extruded outwards, resulting in stress concentration. The structural design of the new rubber cylinder enables the rubber cylinder to fully deform, thereby improving and maintaining the contact stress and obtaining good sealing performance. The deformation of the upper end of the edge rubber cylinder can seal the annular gap in time, thus appropriately improving the differential pressure capacity of the packer.

4. Conclusion

In this paper, the advantages and disadvantages of various hyperelastic models are analyzed. Finally, the Yeoh 3-order model is selected comprehensively, and rubber material parameters under five groups of temperatures are obtained through uniaxial tensile test. The sealing performance of the end-spring rubber cylinder is analyzed through finite element calculation, and it is proved that it can work normally under 65℃~204℃. It provides theoretical and data support for engineering application.

References

[1] Guodong Cui, Zheng Niu, Difei Zhao, Yanlong Kong, et al, High-temperature hydrothermal resource exploration and development: Comparison with oil and gas resource[J], Gondwana Research, 2023,122,306-314

[2] Lei, Q.; Xu, Y.; Cai, B.; Guan, B.; Wang, X.; Bi, G.; Li, H.; Li, S.; Ding, B.; Fu, H.; et al. Progress and prospects of horizontal well fracturing technology for shale oil and gas reservoirs. *Pet. Explor. Dev.* **2022**, *49*, 191–199.

[3] Zhu, Guangyou; Milkov, Alexei V.; Chen, Feiran; et al . Non-cracked oil in ultra-deep high-temperature reservoirs in the Tarim basin, China. Marine and Petroleum Geology, 2018, 89(2), 252-262.

[4] Novy, R.A. Pressure Drops in Horizontal Wells: When Can They Be Ignored? *SPE Res. Eng.* **1995**, *10*, 29–35

[5] Liu Y, Liqin Qian, Jiayan Zou, Chengyu Xia, et al. Study on failure mechanism and sealing performance optimization of

compression packer, Engineering Failure Analysis,2022,1361, 106176.

[6] Wang, P., Cai, M., Liu, Z. et al. Research on key technology of packer rubber barrel for integrated fracturing and completion of gas well[J]. Petrol Explore Prod Technol, 2024,14, 825–838 (2024).

[7] Jin, L., Zhao, D., Liu, J. (2023). A Visco-hyperelastic Constitutive Model for Rubber Considering the Strain Level and One Case Study in the Sealing Packer[J]. Acta Mechanica Solida Sinica, 2023, 36(5), 710–723.

[8] Jin, L; Wang, ZD; Li, RY; et al, Mechanical response of the sealing packer based on two rubber materials at high temperatures[J], POLYMER TESTING, 2023, 124.

[9] Hu, G.; Zhang, P.; Wang, G.; Zhang, M.; Li, M. The influence of rubber material on sealing performance of packing element in compression packer. *J. Nat. Gas Sci. Eng.* **2017**, *38*, 120–138.

[10] Zhang, L;Wen, J;Zhang, H, et al, Mechanical comprehensive evaluation model and sealing performance research of rubber cylinder at large pressure and high temperature[J], PROCEEDINGS OF THE INSTITUTION OF MECHANICAL ENGINEERS PART C-JOURNAL OF MECHANICAL ENGINEERING SCIENCE, 2024, 238(20), 10172-10188

[11] Takahashi S, Okura M, Kobayashi T, et al. Development and verification of degradable sealing elements for fully degradable frac plugs: SPE Asia Pacific Unconventional Resources Conference and Exhibition, Brisbane, Australia, 2015[C].

[12] Wang, P., Cai, M., Liu, Z. et al. Research on key technology of packer rubber barrel for integrated fracturing and completion of gas well[J]. Petrol Explore Prod Technol, 2024, 14, 825–838.

[13] L. Zhang, S. Wang, W. Lv, G.et al , Design and performance research of single rubber cylinder for high pressure gas injection packer[J], Revista Internacional de Métodos Numéricos para Cálculo y Diseño en Ingeniería, 2023, 39(2).

[14] Zhang, L, Zhang, GQ, Wen, J, Yun, et al, Establishment of constitutive model and simulation study on sealing performance of special-shaped rubber cylinder for inner packer in zdeepwater pipeline[J],SO PROCEEDINGS OF THE INSTITUTION OF MECHANICAL ENGINEERS PART C-JOURNAL OF MECHANICAL ENGINEERING SCIENCE, 2024, 238(20), 10127-10142.

[15] Zhang, Y.; Fan, T.; Zhang, P.; Dou, Y. Structural Design and Sealing Performance Analysis of a Nanofluidic Self-Heating Unsealing Rubber Cylinder[J]. Energies, 2023,16, 4890.

[16] Zheng, X.; Li, B. Study on sealing performance of packer rubber based on stress relaxation experiment. *Eng. Fail. Anal.* **2021**, *121*, 105692.

[17] Polonsky V L, Tyurin A P. Design of Packers for Sealing of the Inter-Tube Space in Equipment used for Recovery of Oil and Gas [J]. Chemical & Petroleum Engineering, 2015,51(1-2):37-40.

[18] Lan, WJ., Wang, HX., Zhang, X. et al. Sealing properties and structure optimization of packer rubber under high pressure and high temperature. Pet. Sci.2019, 16, 632–644.

[19] Zheng, X; Li, B; Fei, GS. Evaluation of sealing performance of a compression packer at high temperature[J]. SCIENCE PROGRESS .2022, 105(1):368504221079180.

[20] Liu, Y.; Lian, Z.; Chen, J.; Kuang, S.; Mou, Y.; Wang, Y. Design and Experimental Research on Sealing Structure for a Retrievable Packer. Shock. Vib. 2020, 2020, 7695276.